LA-UR-01-4786
Approved for public release; distribution is unlimited.

Title: **Experimental and Theoretical Study of the Residual Product Nuclide Yields in Thin Targets Irradiated with 100-2600 MeV Protons**

Author(s): Yury E. Titarenko, Vyacheslav F. Batyaev, Evgeny I. Karpikhin, Valery M. Zhivun, Alexsander B. Koldobsky, Ruslan D. Mulambetov, Dmitry V. Fischenko, Svetlana V. Kvasova, Vladilen S. Barasehnkov, Stepan G. Mashnik, Richard E. Prael, Arnold J. Sierk, Hideshi Yasuda, Masaki Saito

Submitted to:

http://lib-www.lanl.gov/la-pubs/00818511.pdf

EXPERIMENTAL AND THEORETICAL STUDY OF THE RESIDUAL PRODUCT NUCLIDE YIELDS IN THIN TARGETS IRRADIATED WITH 100–2600 MEV PROTONS

Yury E. Titarenko, Vyacheslav F. Batyaev, Evgeny I. Karpikhin, Valery M. Zhivun, Aleksander B. Koldobsky, Ruslan D. Mulambetov, Dmitry V. Fischenko, Svetlana V. Kvasova
Institute for Theoretical and Experimental Physics, B.Cheremushkinskaya 25, 117259 Moscow, Russia, e-mail: Yury.Titarenko@itep.ru
Vladilen S. Barashenkov
JINR
Stepan G. Mashnik, Richard E. Prael, Arnold J. Sierk
Los Alamos National Laboratory, Los Alamos, NM 87545, USA
Hideshi Yasuda
Japan Atomic Energy Research Institute, Tokai, Ibaraki, 319-1195, Japan
Masaki Saito
Tokyo Institute of Technology 2-12-1, O-okayama, Meguro-ku, Tokyo 152, Japan

August 10, 2001

ABSTRACT

The work is aimed at measurements and computer simulations of independent and cumulative yields of residual product nuclei in thin targets relevant as target materials and structure materials for hybrid accelerator-driven systems coupled to high-energy proton accelerators [1].

Over 4000 yields of residual nuclides produced in 48 different thin targets (^{182,183,184,186,nat}W, ^{56}Fe, ^{58}Ni, ^{93}Nb, ^{232}Th, ^{nat}U, ^{99}Tc, ^{59}Co, ^{63,65}Cu, ^{nat}Hg, ^{208}Pb, and ^{27}Al) irradiated with 0.1–2.6 GeV protons were determined using the ITEP U-10 synchrotron.

Some of the results have been compared with the data obtained elsewhere, in particular with the recent GSI inverse kinematics experiments [2].

The measured data are compared with the simulations by the LAHET, CEM95, CEM2k, CASCADE, CASCADE/INPE, YIELDX, HETC, and INUCL codes.

Introduction

The values of the yields of residual product nuclei in the medium- and high-energy proton-irradiated thin targets are extensively used in various fundamental and applied researches. The yield values are used to optimize the isotope production in accelerators, to design, develop, and operate high-current accelerators, and to interpret residual product nuclide yields formed in meteorites by cosmic ray-induced nuclear reactions. The yields of residual product nuclei are used also in astrophysics and medicine.

In recent years, the residual product yield data have been widely adopted in the feasibility analyses of accelerator-driven systems (ADS) applicable, for instance, to nuclear waste transmutation [1]. This is related primarily to the information on the applicability scope of the various simulation codes used to calculate high-energy interactions in the ADS structure elements with a view to more reliable calculations of the ADS nuclear parameters and performances.

Table 1 lists the proton energies and the target materials studied under the Project.

Experimental techniques

The samples of 10.5 mm diameter were irradiated by the external proton beam from the ITEP U-10 synchrotron [5]. The experimental nuclide yields were determined by the direct γ-spectrometry method. The γ-spectrometer resolution is of 1.8 keV at the 1332 keV γ-line. The experimental γ-spectra were processed by the GENIE2000 code. The γ-lines were identified, and the cross sections calculated, by the ITEP-developed SIGMA code using the PCNUDAT database. The proton fluence was monitored by the ^{27}Al(p,x)^{22}Na reac-

Table 1: Target materials and proton energies

Target	Proton energy (GeV)						
	0.1	0.2	0.8	1.0	1.2	1.6	2.6
^{182}W		√	√			√	
^{183}W		√	√			√	
^{184}W		√	√			√	
^{186}W		√	√			√	
^{232}Th	√	√	√		√	√	
^{nat}U	√	√	√		√	√	
^{99}Tc	√	√	√		√	√	
^{59}Co		√			√	√	√
^{63}Cu		√			√	√	√
^{65}Cu		√			√	√	√
^{nat}Hg	√	√	√				√
^{56}Fe							√
^{58}Ni							√
^{93}Nb							√
^{nat}W							√
^{208}Pb				√			

tion. More detailed experimental technique description can be found in [3] and [4].

Basic definitions and computational relations

The formalism of representing the reaction product yields (cross sections) in high-energy proton-irradiated thin targets is described in sufficient detail in [5]. In terms of the formalism, the variations in the concentration of any two chain nuclides produced in an irradiated target ($N_1 \xrightarrow{\lambda_1} N_2 \xrightarrow{\lambda_2}$) may be presented to be a set of differential equations that describe the production and decays of the nuclides. By introducing a formal representation of the time functions of the type $F_i = \left(1 - e^{-\lambda_i \tau}\right) \frac{1 - e^{-\lambda_i KT}}{1 - e^{-\lambda_i T}}$, (i=1, 2, Na; τ is the duration of accelerated proton pulse; T is the pulse repetition period; k is the number of pulses within the irradiation period), which characterize the nuclide decays within the irradiation time, and by expressing (similar to the relative measurements) the proton fluence size via monitor reaction cross section σ_{st}, we can present the unknowns as

$$\sigma_1^{cum} = \frac{A_0}{\eta_1 \varepsilon_1 F_1 N_{Na}} \frac{N_{Al}}{N_T} \frac{F_{Na}}{\lambda_{Na}} \sigma_{st}, \qquad (1)$$

$$\sigma_1^{cum} = \frac{A_1}{\nu_1 \eta_2 \varepsilon_2 F_1 N_{Na}} \frac{N_{Al}}{N_T} \frac{\lambda_2 - \lambda_1}{\lambda_2} \frac{F_{Na}}{\lambda_{Na}} \sigma_{st}, \qquad (2)$$

$$\sigma_2^{ind} = \left(\frac{A_2}{F_2} + \frac{A_1}{F_1}\frac{\lambda_1}{\lambda_2}\right) \frac{1}{\eta_2 \varepsilon_2 N_{Na}} \frac{N_{Al}}{N_T} \frac{F_{Na}}{\lambda_{Na}} \sigma_{st}, \qquad (3)$$

$$\begin{aligned} \sigma_2^{cum} &= \sigma_2^{ind} + \nu_1 \sigma_1^{cum} = \\ &= \left(\frac{A_1}{F_1} + \frac{A_2}{F_2}\right) \frac{1}{\eta_2 \varepsilon_2 N_{Na}} \frac{N_{Al}}{N_T} \frac{F_{Na}}{\lambda_{Na}} \sigma_{st} \ , \end{aligned} \qquad (4)$$

where σ_1^{cum} is the cumulative cross section of the first nuclide; σ_2^{ind} and σ_2^{cum} are the independent and cumulative cross sections of the second nuclide; N_{Al} and N_T are the numbers of nuclei in the monitor (standard) and in experimental sample, respectively; η_1 and η_2 are the γ-line yields; ε_1 and ε_2 are the spectrometer efficiencies at energies E_{γ_1} and E_{γ_2}; ν_1 is the branching ratio of the first nuclide; λ_1, λ_2, λ_{Na} are, respectively, the decay constants of the first and second nuclides and of the monitor product (^{22}Na and/or ^{24}Na).

The factors A_0, A_1, and A_2 are calculated through fitting the measured counting rates in the total absorption peaks, which correspond to energies E_{γ_1} (the first nuclide) and E_{γ_2} (the second nuclide), by exponential functions. It should be noted that formulas (1)–(4) were deduced on assumption that the γ- intensities of two nuclides produced under irradiation are recorded up to the desired accuracy within a period from irradiation end to the moment of the ultimate detectable intensity. If, for some reasons, the factor A_1 cannot be found, then the factor A_2 will be used together with expression (14) from [5] to determine the constant ($\sigma_2^{cum^*}$), which may be called the supra cumulative yield:

$$\begin{aligned} \sigma_2^{cum^*} &= \sigma_2 + \frac{\lambda_2}{\lambda_1 - \lambda_2} \nu_1 \sigma_1^{cum} = \\ &= \frac{A_2}{\eta_2 \varepsilon_2 F_2 N_{Na}} \frac{N_{Al}}{N_T} \frac{F_{Na}}{\lambda_{Na}} \sigma_{st} \ . \end{aligned} \qquad (5)$$

The resultant value may prove to be very different from σ_2^{cum}. Nevertheless, the supra-cumulative yield can be either used directly to verify the codes, or determined further up to σ_2^{cum} if the latter is obtained elsewhere (for example in the inverse kinematics experiments).

Experimental results

More than four thousand yields of reaction products in the targets listed in Table 1 are detremined and presented in our Report [3]. Table 2 shows the total amount of measured reaction product yields of different types in each of our measurement.

Simulation of experimental data

The work is aimed also at verifying the simulation codes used most extensively in ADS applications in order to estimate their predictive abilities and to stimulate efforts to improve them.

Table 2: Number of measured reaction product yields of different types in each experiment

Experiment		Yield type					Total
Target	E_p [GeV]	i	c	c^*	$i_{\Sigma m_j}$	$i_{\Sigma m_j+g}$	
^{182}W	0.2	3	22	3	1	3	32
^{182}W	0.8	5	52	6	1	6	70
^{182}W	1.6	10	84	3	6	6	109
^{183}W	0.2	4	23	3	1	4	35
^{183}W	0.8	6	55	6	2	7	76
^{183}W	1.6	12	84	3	6	6	111
^{184}W	0.2	4	23	3	1	5	36
^{184}W	0.8	7	55	6	2	7	77
^{184}W	1.6	12	85	3	7	7	114
^{186}W	0.2	4	23	3	1	5	36
^{186}W	0.8	4	48	5	1	4	62
^{186}W	1.6	13	87	3	8	8	119
^{nat}W	2.6	10	100	4	9	6	129
^{232}Th	0.1	10	58	2	9	8	87
^{232}Th	0.2	16	80	4	18	10	128
^{232}Th	0.8	15	78	11	15	11	130
^{232}Th	1.2	22	140	13	19	20	214
^{232}Th	1.6	22	143	13	18	16	212
^{nat}U	0.1	12	74	3	9	10	108
^{nat}U	0.2	15	77	3	15	13	123
^{nat}U	0.8	21	122	15	17	20	195
^{nat}U	1.2	22	146	15	22	21	226
^{nat}U	1.6	23	151	15	22	20	231
^{99}Tc	0.1	4	9	0	3	2	18
^{99}Tc	0.2	4	21	0	9	5	39
^{99}Tc	0.8	10	40	3	11	8	72
^{99}Tc	1.2	8	39	2	12	6	67
^{99}Tc	1.6	10	44	3	11	10	78
^{59}Co	0.2	6	17	0	3	3	29
^{59}Co	1.2	7	26	0	4	4	41
^{59}Co	1.6	7	26	0	4	4	41
^{59}Co	2.6	7	26	0	4	4	41
^{63}Cu	0.2	9	12	1	3	4	29
^{63}Cu	1.2	10	27	2	4	4	47
^{63}Cu	1.6	11	22	1	4	4	42
^{63}Cu	2.6	11	22	1	4	4	42
^{65}Cu	0.2	8	13	1	4	3	29
^{65}Cu	1.2	13	29	2	5	5	54
^{65}Cu	1.6	10	26	1	5	5	47
^{65}Cu	2.6	10	27	1	5	5	48
^{nat}Hg	0.1	4	17	1	10	12	44
^{nat}Hg	0.2	6	27	6	12	14	65
^{nat}Hg	0.8	9	57	11	12	14	103
^{nat}Hg	1.6	8	90	13	16	14	141
^{56}Fe	2.6	5	24	1	3	3	36
^{58}Ni	2.6	9	21	1	3	4	38
^{93}Nb	2.6	6	56	2	12	8	85
^{208}Pb	1.0	8	65	11	15	15	114
	Total	472	2593	209	388	387	4050

i – independent yields of ground states, **c** – cumulative yields,
$\mathbf{c}^*$ – supra-cumulative yields,
$\mathbf{i}_{\Sigma m_j}$ – independent yields of metastable states,
$\mathbf{i}_{\Sigma m_j+g}$ – summed independent yields of metastable and ground states.

The following thirteen codes were used for simulations:

- the CEM95 cascade-exciton model code [6],
- the latest version of the improved cascade-exciton model [7] code, CEM2k, [8],
- the CASCADE cascade-evaporation-fission transport code [9],
- the INUCL cascade-preequilibrium-evaporation-fission code [10],
- the LAHET (both ISABEL and Bertini options) cascade-preequilibrium-evaporation-fission transport code [11],
- the YIELDX semi-phenomenological code [12],
- the CASCADE/INPE cascade-evaporation-preequilibrium-fission-transport code [13].
- the CASCADO-IPPE cascade-evaporation-preequilibrium-fission-transport code [14]
- the GNASH code based on the Hauser-Feshbach and preequilibrium approach [15],
- the ALICE code with HMS precompound approach [16],
- the Quantum Molecular Dynamics (QMD) code [17],
- the NUCLEUS cascade – evaporation – fission code [18],
- the ALICE-IPPE code [19].

Most of the codes used here are described in some detail in [5].

Contrary to the simulated data, the experimental results include not only independent but also (and mainly) cumulative and supra-cumulative residual product nuclei. To get a correct comparison between the experimental and simulation data, the cumulative yields must be calculated on the basis of the simulated independent yields. The procedure of calculation the cumulative yields and comparing experimental and simulation results is described in detail in [4] and [5].

The default options were used in all of the simulation codes without modifying the codes to get optimal agreement with the data. All the calculations were made before any experimental results were obtained, except the results from CEM2k. With such an approach, our comparisons demonstrate the real predictive power, rather than the descriptive power of the codes.

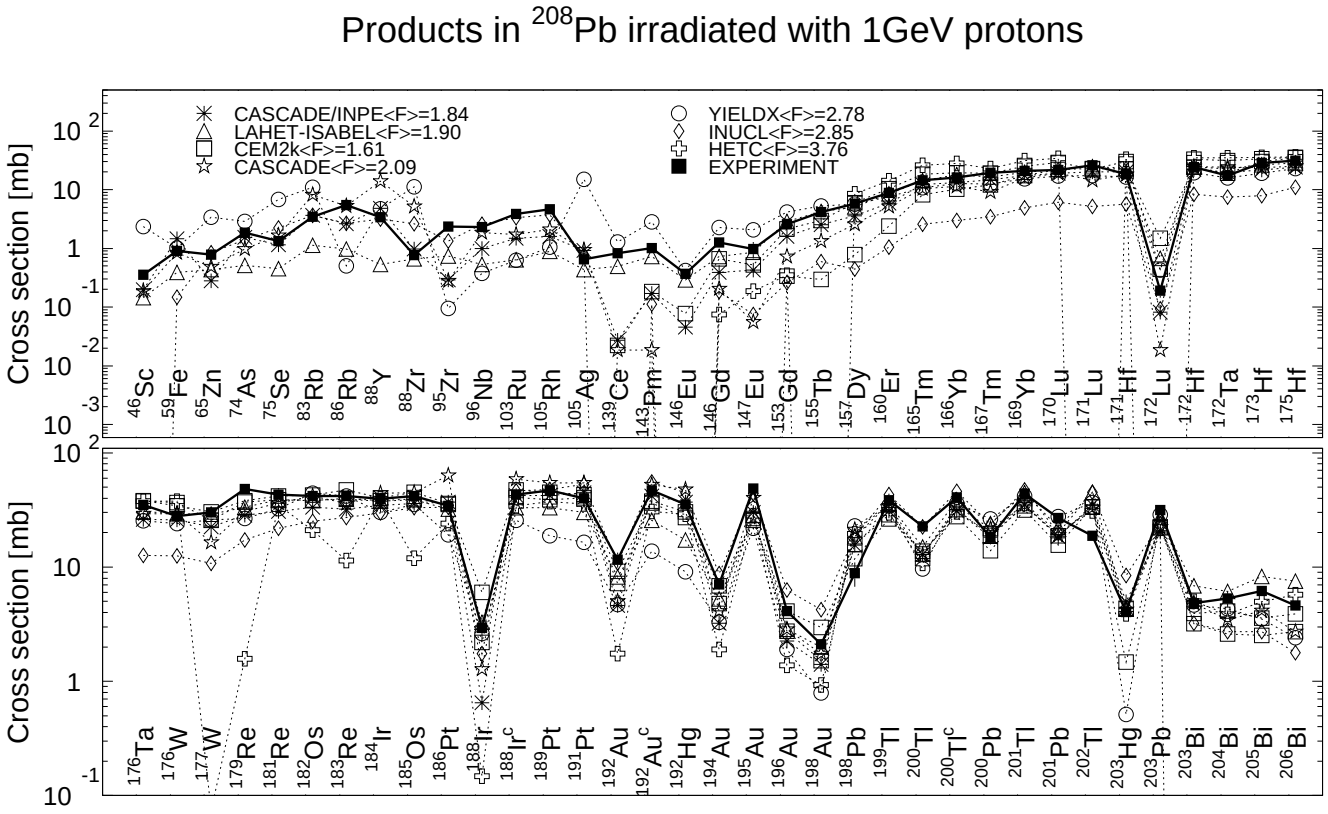

Figure 1: Detailed comparison between experimental and simulated yields of radioactive reaction products. The cumulative yields are labeled with a "c" when the respective independent yields are also shown. The mean simulation-to-experimental data ratios are shown in the legend for each of the codes.

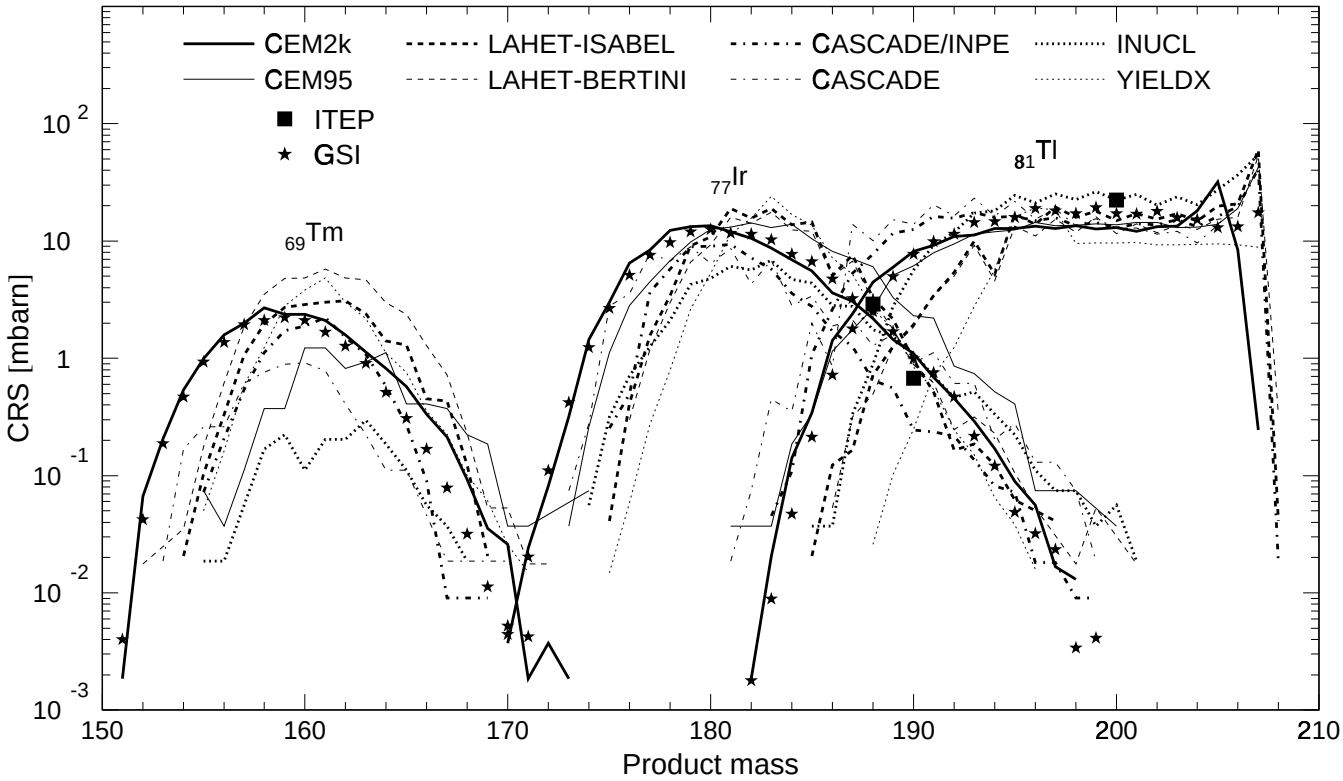

Figure 2: Isotopic mass distribution for independent products of Tm, Ir, and Tl isotopes. Black squares are our measurements, while filled stars show GSI data [2] obtained in reverse kinematics. Results from different codes are marked as indicated.

Comparison of experiment with simulations

Table 3 presents quantitative information concerning the agreement of the simulated yields with experimental data for each of the simulation codes, namely:

- the total number of measured yields, N_E;
- of them, the number of the measured yields selected to compare with calculations, N_G. We reject the following nuclides from our comparison in the cases where:
  1. The measured product is of metastable or just ground state;
  2. There is a transition of a metastable state to a product out of the given decay chain;
  3. There is a strong correlation between a measured cumulative yield decaying into another one; The cumulative yields of the precursors in all the above chains are almost equal to the cumulative yields of the daughters, that is why only the daughter yields were used in our comparison, to prevent double counting. Also, in case of a strong correlation between the cumulative and independent yields of a product, only the independent yield was used for comparison;
- of them, the number of the product nuclei whose yields were simulated by a particular code, N_S;
- the number of comparison events when the simulated results differ from the experimental data by not more than 30%, $N_{C_{1.3}}$, and the number of comparison events when the calculations differ from data by not more than a factor of 2.0, $N_{C_{2.0}}$;
- the mean squared deviation of the simulated results from experimental data, $< F >$, and its standard deviation, $S(< F >)$.

Summary on the agreement between the experimental and simulated product nuclide yields

It is expedient to make comparison for two groups of nuclei: with a significant fission mode (conditionally "heavy" nuclei, ^{182,183,184,186,nat}W, ^{nat}Hg, ^{208}Pb, ^{232}Th, and ^{nat}U) and without any fission mode (conditionally "light" nuclei, ^{56}Fe, ^{58}Ni, ^{59}Co, ^{63,65}Cu, ^{93}Nb, and ^{99}Tc). It should be noted that, beside a methodological convenience, this classification reflects (somewhat conditionally) the distinquishing design features of the materials as applied to the ADS (the target and structure materials). 2427 yields of 4050 yields obtained were used to verify the simulation codes. Table 3 and Figure 4 summarize the information on the predictive power of the codes.

In the case of light nuclei, where nearly all product nuclides are formed by spallation, the predictive power of most of the Monte-Carlo codes is characterized by the mean squared deviation factor of at least 2, with the agreement being somewhat worse at low energies. The semi-phenomenological code YIELDX gives the best result when predicting the reaction product yields in light nuclei, and sometimes approaches the required 30% accuracy. It should be noted, however, that YIELDX does not use any physical model, but is based on approximations for a large set of experimental data.

In the case of heavy nuclei, the physics of proton-nucleus interactions gets complicated because the fission process becomes significant. Production of high-energy fission product nuclides is not considered by some of the tested codes (CEM95, CEM2k, HETC) and the applied in other codes fission models are imperfect. Therefore, the mean squared deviation factor (see Table 4) is very high (commonly, at least 3.0 and sometimes about an order of magnitude) for the fission products. From this it follows that, although the spallation products are described by the present-day codes somewhat better for heavy nuclei that for light nuclei (the mean squared deviation factor of about 1.5), the general agreement is about the same as in the case of light nuclei (the mean squared deviation factor about 2.0 and higher). Our study shows that further development of reliable fission models is a priority task in updating all the codes tested here.

It should be also noted that, in the case of high-energy (E_p >1 GeV) projectile protons, most of the tested codes fail to satisfactorily describe the production of the nuclides whose nucleon compositions are close to the primary nuclei. This is also true at intermediate incident energies, indicating on the imperfectnees of the physical models used to describe $(p, xpyn)$–type processes, where $x+y \leq 3$ (the pre-equilibrium nucleon emission).

As a whole, it can be concluded that almost all the above-verified codes are applicable, during the stage of feasibility study and development work, but are not yet reliable enough to solve applied problems that arise when designing and operating ADS facilities. At the same time, the yields of numerous secondary products have to be known to within a very high accuracy for many reasons (large cross sections for neutron capture,

Table 3: Statistics of the simulation-to-experiment comparisons of the yields of the all presented reaction products

Code	^{59}Co,^{63,65}Cu, E$_p$=0.2GeV ^{99}Tc, E$_p$ ≤0.2GeV N_E=144 N_G=76			^{59}Co,^{63,65}Cu, ^{59}Fe, ^{58}Ni, ^{93}Nb, E$_p$ ≥1.2GeV ^{99}Tc, E$_p$ ≥0.8GeV N_E=779 N_G=515		
	$N_{1.3}/N_{2.0}/N_S$	$\langle F\rangle$	$S(\langle F\rangle)$	$N_{1.3}/N_{2.0}/N_S$	$\langle F\rangle$	$S(\langle F\rangle)$
CEM95	23/42/69	3.04	2.39	136/273/468	2.57	1.94
LAHET	26/52/72	2.03	1.60	154/346/478	2.03	1.62
INUCL	18/45/76	2.72	2.00	112/283/479	2.47	1.84
HETC	7/19/50	4.37	2.51	81/162/308	3.81	2.85
CASCADE	11/32/75	3.40	2.15	107/260/483	2.71	1.96
YIELDX	21/52/76	2.02	1.55	219/417/504	1.75	1.50
NUCLEUS	–	–	–	6/15/28[1]	2.21	1.52
QMD	–	–	–	15/46/81[2]	2.99	2.06
GNASH	3/ 3/ 7[3]	2.74	1.89	–	–	–
ALICE(Kat)	2/3/12[3]	2.77	1.66	–	–	–
ALICE(Fer)	2/6/12[3]	2.31	1.60	–	–	–
Code	^{182,3,4,6}W,^{nat}Hg, E$_p$ ≤0.2GeV ^{232}Th,^{nat}U, E$_p$ ≤0.2GeV N_E=694 N_G=395			^{182,3,4,6,nat}W,^{nat}Hg, ^{208}Pb, E$_p$ ≥0.8GeV ^{232}Th,^{nat}U, E$_p$ ≥0.8GeV N_E=2433 N_G=1441		
	$N_{1.3}/N_{2.0}/N_S$	$\langle F\rangle$	$S(\langle F\rangle)$	$N_{1.3}/N_{2.0}/N_S$	$\langle F\rangle$	$S(\langle F\rangle)$
CEM95	65/105/147[4]	2.34	2.01	321/503/585[5]	1.90	1.77
LAHET	164/305/386	1.95	1.69	399/945/1334	2.04	1.62
INUCL	75/171/375	4.19	2.73	293/619/1213	4.05	2.92
HETC	39/74/128[4]	3.20	2.52	221/422/560[5]	2.88	2.55
CASCADE	78/176/379	5.46	3.53	451/828/1322	3.05	2.42
YIELDX	54/94/131[6]	2.03	1.65	201/443/732[5]	2.37	1.78
CASCADO^{IPPE}	34/63/97[7]	2.88	2.33	35/109/180[8]	2.73	2.01
ALICE-IPPE	1/8/16[9]	3.27	2.10	–	–	–
CEM2k	24/45/55[10]	1.64	1.40	91/198/235[11]	2.02	1.74
CASCADE^{INPE}	–	–	–	27/51/64[12]	1.84	1.56

[1] Here N_E=41 and N_G=29.
[2] Here N_E=152 and N_G=105.
[3] Here N_E=39 and N_G=12,
[4] Here N_E=248 and N_G=160.
[5] Here N_E=1225 and N_G=742.
[6] Here N_E=204 and N_G=133.
[7] Here N_E=195 and N_G=102.
[8] Here N_E=325 and N_G=186.
[9] Here N_E=195 and N_G=112.
[10] Here N_E=111 and N_G=66.
[11] Here N_E=552 and N_G=291.
[12] Here N_E=114 and N_G=70.

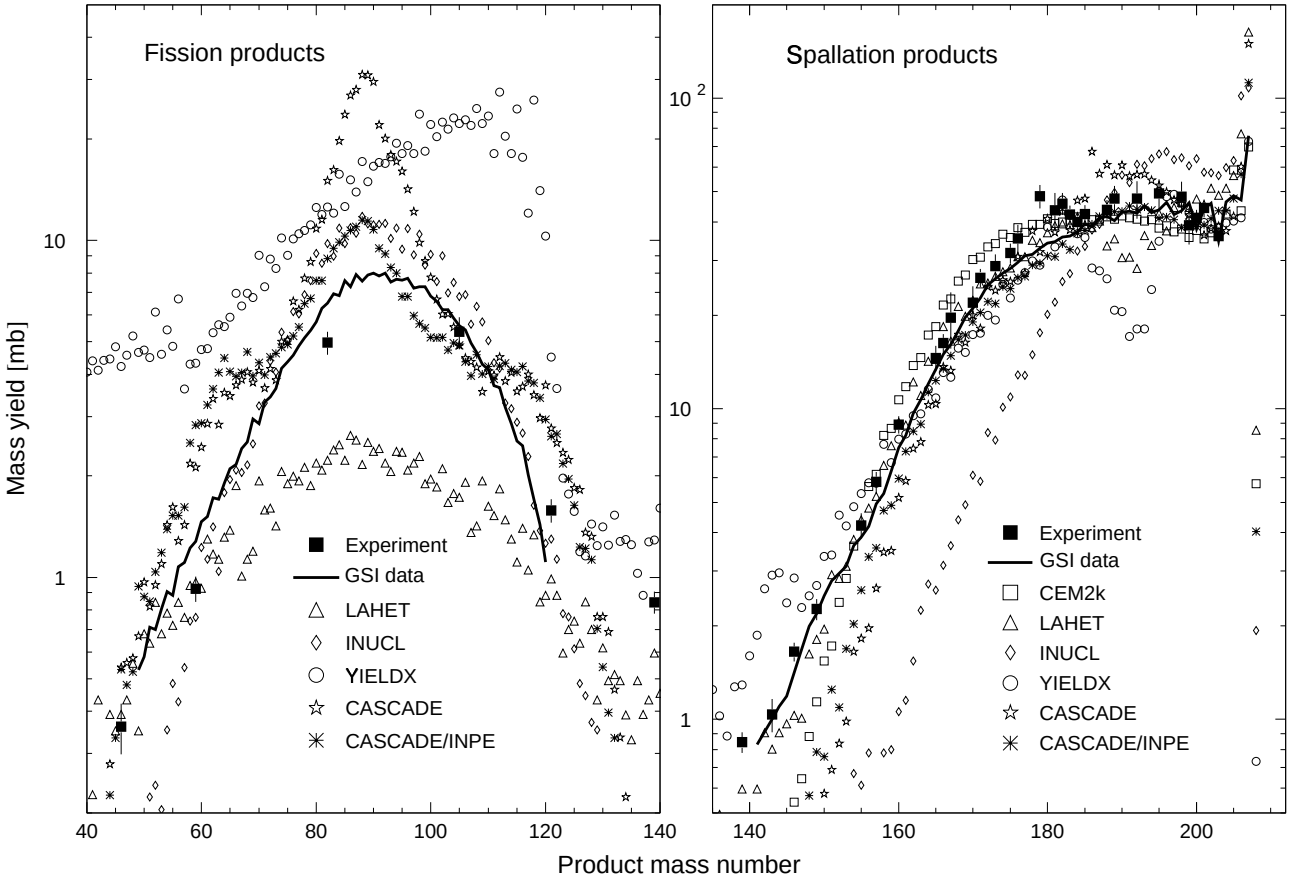

Figure 3: The simulated mass distributions of reaction products together with the measured cumulative and supra-cumulative yields. Black line shows GSI data in reverse kinematics [2].

a high radiotoxicity, chemical poisoning of structure elements, gas evolution, etc.). So, the codes have to be further improved to become a reliable tool for calculating ADS parameters.

Methods for improving the simulation codes

Most of the simulation codes for intermediate-energy nuclear reactions use the Monte-Carlo method, are based on Intranuclear Cascade (INC) models, and treat a reaction as a multistage process (INC, preequilibrium, equilibrium evaporation, and fission).

Since the intermediate energy range is very broad, different models are applied in different regions to describe different stages of a reaction. The models describe these stages with different degree of rigor and are of different predictive powers. As a result, the simulation results by different codes (similar by the physical processes involved) differ significantly from each other.

The accuracy of describing the experimental yields of nuclear reaction products, as well as the predictive power of simulation codes, can well be improved by updating the models realized in the codes via solving a number of fundamental problems, of which the following are of most importance:

- Development of a consistent nuclear fission model that would allow for the shell-to-liquid drop fission barrier transition and for the nuclear viscosity effects;
- Updating the INC models and improvement in description of complex particle and cluster emission during the preequilibrium and evaporation stages of nuclear reactions;
- Improvement the calculation of inverse cross sections and level densities used at both preequilibrium and evaporation stages of reactions;
- Development of consistent methods to calculate the spallation reaction cross sections and comparing the INC model predictions with optical-statistical calculations in order to correctly include the nuclear structure effects in the energy range of 20–200 MeV.

Table 4: Statistics of the experimental-to-simulated spallation and fission yield comparisons

Code	**Spallation**			**Fission**			**All products** (spallation+fission+frag-mentation)		
^{208}Pb	N_T = 74, N_G = 55			N_T = 30, N_G = 15			N_T = 114, N_G = 70		
E_p=1.0GeV	$N_{1.3}/N_{2.0}/N_S$	$\langle F\rangle$	S($\langle F\rangle$)	$N_{1.3}/N_{2.0}/N_S$	$\langle F\rangle$	S($\langle F\rangle$)	$N_{1.3}/N_{2.0}/N_S$	$\langle F\rangle$	S($\langle F\rangle$)
LAHET	36/51/55	1.39	1.31	1/3/15	3.65	1.70	36/55/70	1.92	1.73
CEM2k	33/53/55	1.40	1.25	–	–	–	33/54/60	1.62	1.45
CASCADE/INPE	26/47/51	1.52	1.34	4/9/15	2.24	1.70	32/56/70	1.85	1.59
CASCADE	24/46/54	1.61	1.37	5/9/15	2.59	1.94	29/55/72	2.18	1.88
YIELDX	23/42/55	1.82	1.53	1/3/15	7.04	2.57	27/49/76	2.76	2.24
CEM95	30/46/55	2.17	2.03	–	–	–	30/46/55	2.16	2.00
INUCL	16/27/55	2.75	1.99	7/11/14	1.95	1.71	24/40/73	2.89	2.15
^{nat}W	N_T = 100, N_G = 61			N_T = 17, N_G = 14			N_T = 129, N_G = 81		
E_p=2.6GeV	$N_{1.3}/N_{2.0}/N_S$	$\langle F\rangle$	S($\langle F\rangle$)	$N_{1.3}/N_{2.0}/N_S$	$\langle F\rangle$	S($\langle F\rangle$)	$N_{1.3}/N_{2.0}/N_S$	$\langle F\rangle$	S($\langle F\rangle$)
CEM95	31/56/61	1.53	1.36	–	–	–	31/57/69	2.40	2.20
CASCADE	37/54/61	1.54	1.42	2/4/13	5.43	3.12	39/61/79	2.26	2.07
CEM2k	18/51/61	1.71	1.34	–	–	–	19/55/71	2.10	1.65
LAHET	11/49/61	1.81	1.35	0/3/11	6.36	2.97	11/53/77	2.51	1.90
YIELDX	22/40/61	1.88	1.47	3/8/14	2.30	1.70	25/51/81	2.04	1.56
INUCL	28/49/61	2.06	1.82	0/0/5	14.16	1.86	28/49/70	3.43	2.88
^{nat}Hg	N_T = 36, N_G = 24			N_T = 8, N_G = 5			N_T = 44, N_G = 29		
E_p=0.1GeV	$N_{1.3}/N_{2.0}/N_S$	$\langle F\rangle$	S($\langle F\rangle$)	$N_{1.3}/N_{2.0}/N_S$	$\langle F\rangle$	S($\langle F\rangle$)	$N_{1.3}/N_{2.0}/N_S$	$\langle F\rangle$	S($\langle F\rangle$)
CEM2k	6/18/23	1.73	1.36	–	–	–	6/18/23	1.73	1.36
LAHET	8/16/23	1.78	1.43	0/0/3	7.88	1.45	8/16/26	2.43	1.92
INUCL	8/15/23	2.12	1.64	0/0/4	6.97	1.77	8/15/27	2.77	2.02
CASCADE	12/16/23	2.15	1.88	0/2/4	3.77	2.07	12/18/27	2.39	1.99
CEM95	8/14/24	2.19	1.68	–	–	–	8/14/24	2.19	1.68
^{nat}Hg	N_T = 52, N_G = 35			N_T = 13, N_G = 7			N_T = 65, N_G = 42		
E_p=0.2GeV	$N_{1.3}/N_{2.0}/N_S$	$\langle F\rangle$	S($\langle F\rangle$)	$N_{1.3}/N_{2.0}/N_S$	$\langle F\rangle$	S($\langle F\rangle$)	$N_{1.3}/N_{2.0}/N_S$	$\langle F\rangle$	S($\langle F\rangle$)
LAHET	17/30/35	1.50	1.30	0/1/6	3.70	1.74	17/31/41	1.87	1.60
CEM2k	20/29/35	1.59	1.41	–	–	–	20/29/35	1.59	1.41
YIELDX	15/31/35	1.59	1.33	0/3/7	2.55	1.47	15/34/42	1.77	1.43
CASCADE	10/28/35	2.09	1.75	2/3/6	3.36	2.26	12/31/41	2.28	1.87
CEM95	12/28/35	2.13	1.84	–	–	–	12/28/35	2.13	1.84
INUCL	10/21/35	2.22	1.69	2/2/6	2.66	1.77	12/23/41	2.29	1.71
^{nat}Hg	N_T = 66, N_G = 47			N_T = 21, N_G = 13			N_T = 103, N_G = 70		
E_p=0.8GeV	$N_{1.3}/N_{2.0}/N_S$	$\langle F\rangle$	S($\langle F\rangle$)	$N_{1.3}/N_{2.0}/N_S$	$\langle F\rangle$	S($\langle F\rangle$)	$N_{1.3}/N_{2.0}/N_S$	$\langle F\rangle$	S($\langle F\rangle$)
CASCADE	26/43/46	1.43	1.26	4/7/12	2.49	1.85	31/51/66	2.33	2.08
LAHET	31/44/47	1.45	1.32	1/1/12	3.97	1.58	36/54/69	1.96	1.71
CEM2k	23/45/47	1.45	1.26	–	–	–	24/47/54	1.73	1.51
CEM95	33/44/47	1.54	1.50	–	–	–	33/44/51	2.30	2.28
YIELDX	18/37/47	1.68	1.36	4/5/13	3.29	2.08	27/51/70	2.09	1.72
INUCL	22/34/46	1.88	1.57	2/3/11	4.36	2.28	24/37/65	2.68	2.02
^{nat}Hg	N_T = 92, N_G = 61			N_T = 30, N_G = 21			N_T = 141, N_G = 90		
E_p=2.6GeV	$N_{1.3}/N_{2.0}/N_S$	$\langle F\rangle$	S($\langle F\rangle$)	$N_{1.3}/N_{2.0}/N_S$	$\langle F\rangle$	S($\langle F\rangle$)	$N_{1.3}/N_{2.0}/N_S$	$\langle F\rangle$	S($\langle F\rangle$)
CASCADE	38/56/61	1.50	1.37	5/11/17	2.04	1.49	44/73/86	1.64	1.44
CEM95	36/56/61	1.52	1.38	–	–	–	37/59/68	1.88	1.74
LAHET	12/49/60	1.73	1.26	5/10/19	2.63	1.87	17/63/87	2.00	1.48
CEM2k	17/51/61	1.73	1.36	–	–	–	22/58/73	2.40	2.03
INUCL	21/50/61	1.87	1.58	4/9/16	2.85	2.04	26/61/85	2.43	1.97
YIELDX	15/45/61	2.01	1.55	3/7/20	3.65	1.98	19/55/89	2.45	1.76

It should be noted that the parametric fittings (phenomenological systematicls) in the present-day codes like YIELDX do not reach sufficient accuracy in representing the basic physical effects, therefore can but only partly solve the problem of providing the needed cross sections. In some cases, such a fitting can distort the parameters and their physical sense, thereby considerably restricting the predictive power of such codes.

Acknowledgments

The authors are indebted to Drs. T. Enqvist and B. Mustapha for providing us the cross sections measured at the GSI, to Prof. R. Michel for sending us the nuclide production data obtained at the ZSR, to Dr. F. E. Chukreev for helpful comments on the nuclear decay-chain data, and to Prof. V. Artisyuk for useful discussions and help. Also we thank Drs. S. Chiba, H. Takada, M. Blann, M. Chadwick, T. Gabriel,

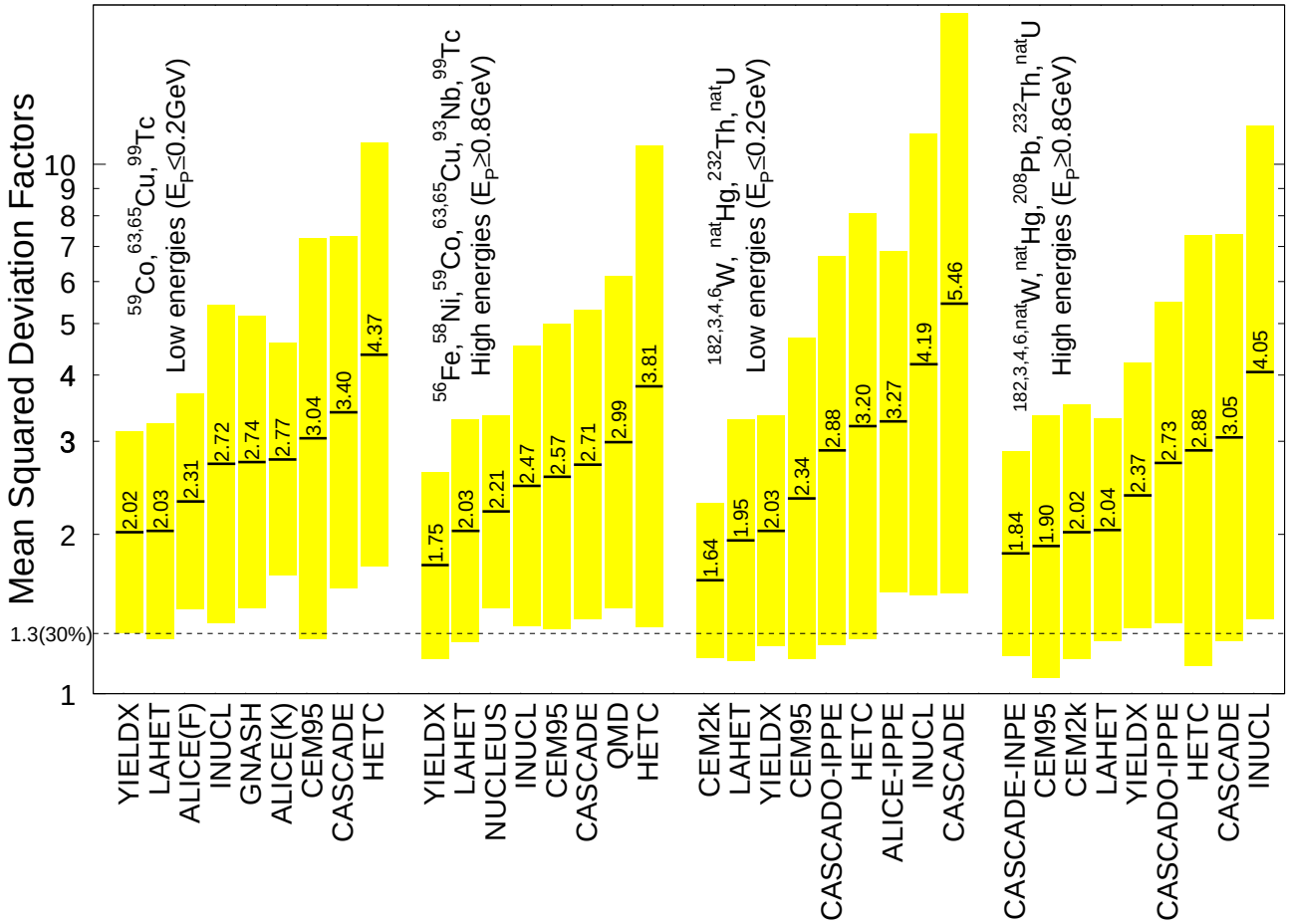

Figure 4: The mean squared deviation factor for the unified comparison.

Yu. N. Shubin, and A. V. Ignatyuk for the theoretical calculations performed via their codes.

The work has been performed under the ISTC Project #839 supported by the European Community, Japan (JAERI), and Norway and was partially supported by the U. S. Department of Energy.

REFERENCES

[1] G. Van Tuyle and D.E. Beller, "Accelerator Transmutation of Waste Technology and Implementation Scenarios," Proc. of the Third International Topical Meeting on Nuclear Applications of Accelerator Technology (AccApp'99), Long Beach, California, November 14-18, 1999, pp. 337-346.

[2] W. Wlazlo, T. Enqvist, P. Armbruster, J. Benlliure, M. Bernas, A. Boudard, S. Czájkowski, R. Legrain, S. Leray, B. Mustapha, M. Pravikoff, F. Rejmund, K.-H. Schmidt, C. Stéphan, J. Taieb, L. Tassan-Got, and C. Volant, Phys. Rev. Lett. **84**, 5736 (2000); T. Enqvist, W. Wlazlo, P. Armbruster, J. Benlliure, M. Bernas, A. Boudard, S. Czájkowski, R. Legrain, S. Leray, B. Mustapha, M. Pravikoff, F. Rejmund, K.-H. Schmidt, C. Stéphan, J. Taieb, L. Tassan-Got, and C. Volant, "Isotopic Yields and Kinematic Energies of Primary Residues in 1*A* GeV ^{208}Pb + p Reactions," Nucl. Phys. **A686**, 481 (2001).

[3] Yuri E. Titarenko, Final Project Technical Report of ISTC 839B-99 "Experimental and Theoretical Study of the Yields of Residual Product Nuclei Produced in Thin Targets Irradiated by 100–2600 MeV Protons, ISTC 833B-99, Moscow, Russia (February 2001).

[4] Yu.E. Titarenko, O.V. Shvedov, V.F. Batyaev, E.I. Karpikhin, V.M. Zhivun, A.B. Koldobsky, R.D. Mulambetov, D.V. Fischenko, S.V. Kvasova, A.N. Sosnin, S.G. Mashnik, R.E. Prael, A.J. Sierk, T.A. Gabriel, M. Saito, and H. Yasuda, "Cross Sections for Nuclide Production in 1 GeV Proton-irradiated Pb", Los Alamos National Laboratory Report LA-UR-00-4779, Los Alamos (2000), E-print *nucl-th/0011083*, submitted to *Phys. Rev. C.*

[5] Yu. E. Titarenko, O. V. Shvedov, M. M. Igumnov, S. G. Mashnik, E. I. Karpikhin, V.D. Kazaritsky, V. F. Batyaev, A. B. Koldobsky, V. M. Zhivun, A.N. Sosnin, R. E. Prael, M. B. Chadwick, T. A. Gabriel, M. Blann, "Exerimental and theoretical Study of the Yields of Radionuclides Produced in 209Bi thin target Irradiated by 1500 MeV and 130MeV Protons", Nucl. Instr. and Meth. A414 (1998)73-99.

[6] K. K. Gudima, S. G. Mashnik, and V. D. Toneev, Nucl. Phys. A **401**, 329 (1983); S. G. Mashnik, "User Manual for the Code CEM95", JINR, Dubna, 1995; OECD Nuclear Energy Agency Data Bank, Paris, France, 1995; http://www.nea.fr/abs/html/iaea1247.html; RSIC-PSR-357, Oak Ridge, 1995.

[7] S. G. Mashnik and A. J. Sierk, in *Proceedings of the Fourth International Workshop on Simulating Accelerator Radiation Environments (SARE4), Knoxville, TN, 1998*, edited by T. A. Gabriel, (ORNL, 1999), p. 29.

[8] S. G. Mashnik and A. J. Sierk, "CEM2k - Recent Developments in CEM," in *Proc. of the Fourth International Topical Meeting on Nuclear Applications of Accelerator Technology (AccApp00), November 13-15, 2000, Washington, DC, USA*, (American Nuclear Society, La Grange Park, IL, USA, 2001) pp. 328-341; http://xxx.lanl.gov/ps/nucl-th/001164.

[9] V. S. Barashenkov, Le Van Ngok, L. G. Levchuk, Zh. Zh. Musul'manbekov, A. N. Sosnin, V. D. Toneev, and S. Yu. Shmakov, JINR Report R2-85-173, Dubna, 1985; V. S. Barashenkov, F. G. Zheregi, and Zh. Zh. Musul'manbekov, Yad. Fiz. **39**, 1133 (1984) [Sov. J. Nucl. Phys. **39**, 715 (1984)]; V. S. Barashenkov, B. F. Kostenko, and A. M. Zadorogny, Nucl. Phys. A **338**, 413 (1980).

[10] G. A. Lobov, N. V. Stepanov, A. A. Sibirtsev, and Yu. V. Trebukhovskii, Institute for Theoretical and Experimental Physics (ITEP) Preprint No. ITEP-91, Moscow, 1983; A. A. Sibirtsev, N. V. Stepanov, and Yu. V. Trebukhovskii, ITEP Preprint No. ITEP-129, Moscow, 1985; N. V. Stepanov, ITEP Preprint No. ITEP-81, Moscow, 1987; N. V. Stepanov, ITEP Preprint No. ITEP-55-88, Moscow, 1988 (in Russian).

[11] R. E. Prael and H. Lichtenstein, "User guide to LCS: The LAHET Code System," Los Alamos National Laboratory Report No. LA-UR-89-3014 (1989); see also the Web page at: http://www-xdiv.lanl.gov/XTM/lcs/lahet-doc.html.

[12] C. H. Tsao, Private communication; R. Silberberg, C. H. Tsao, and A. F. Barghouty, Astrophys. J., **501**, 911 (1998); R. Silberberg and C. H. Tsao, Astrophys. J. Suppl., No. 220, **25**, 315 (1973); *ibid*, p. 335.

[13] V. S. Barashenkov, A. Yu. Konobeev, Yu. A. Korovin, and V. N. Sosnin, Atomnaya Energiya **87**, 283 (1999) [Atomic Energy **87**, 742 (1999)].

[14] Yu. N. Shubin, Proc. ADDTA'99; A. V. Ignatyuk, N. T. Kulagin, V. P. Lunev, and K.-H. Schmidt, "Analysis of Spallation Residues within the Intranuclear Cascade Model," Proc. XV Workshop on Physics of Nuclear Fission, Obninsk, 3-6 October, 2000.

[15] P.G. Young, E.D. Arthur and M.B.Chadwick, Los Alamos National Laboratory Report LA-12343-MS (1992); M.B. Chadwick and P.G. Young, Phys. Rev. C 47 (1993) 2255.

[16] M. Blann, Phys. Rev. C 54 (1996) 1341; M. Blann and M. B. Chadwick, Phys. Rev. C 57 (1998) 233; M. Blann and M. B. Chadwick, Phys. Rev. C 62 (2000) 034604.

[17] Phys. Rev. C52 (1995) 2620; K. Niita, S. Chiba, H. Takada, and T. Maruyama, Proc. of the Third Workshop on Simulating Accelerator Radiation Environments, KEK Proceedings 97-5 (1997) edited by H. Hirayama, p.1.

[18] T. Nishida, Y. Nakahara, T. Tsutsui: "Development of a Nuclear Spallation Simulation Code and Calculations of Primary Spallation Products", JAERI-M 86-116, (1986), [in Japanese].

[19] A.I. Dityuk, A.Yu. Konobeyev, V.P. Lunev, and Yu.N. Shubin, New Version of the Advanced Computer Code ALICE-IPPE, Report INDC (CCP)-410, IAEA, Vienna, 1998.

[20] R. B. Firestone, in: *Tables of Isotopes, 8th ed.: 1998 Update (with CD ROM)* edited by

S. Y. Frank Chu (CD-ROM Ed.), C. M. Baglin (Ed.), (Wiley Interscince, New York, 1996).

[21] J. R. Letaw, R. Silberberg, and C. H. Tsao, Astrophys. J. Suppl., **51**, 271 (1983).

[22] A. Koning, in *Proceedings of the Second International Conference on Accelerator-Driven Transmutation Technologies and Applications (ADTT'96), Kalmar, Sweeden, 1996*, edited by H. Conde (Uppsala University, Uppsala, 1997), p. 438.